frontiers in Earth Science

ORIGINAL RESEARCH
published: 09 September 2021
doi: 10.3389/feart.2021.697388

Hydrogeochemistry and Acidic Property of Submarine Groundwater Discharge Around Two Coral Islands in the Northern South China Sea

Hon-Kit Lui[1], Min-Yun Liu[2], Hsiu-Chin Lin[3], Hsiao-Chun Tseng[4], Li-Lian Liu[1,5], Feng-Yu Wang[2], Wei-Ping Hou[2], Rae Chang[1] and Chen-Tung Arthur Chen[1]**

[1]Department of Oceanography, National Sun Yat-sen University, Kaohsiung, Taiwan, [2]Taiwan Ocean Research Institute, National Applied Research Laboratories, Kaohsiung, Taiwan, [3]Department of Marine Biotechnology and Resources, National Sun Yat-sen University, Kaohsiung, Taiwan, [4]Institute of Marine Environment and Ecology, National Taiwan Ocean University, Keelung, Taiwan, [5]Frontier Center for Ocean Science and Technology, National Sun Yat-sen University, Kaohsiung, Taiwan

OPEN ACCESS

Edited by:
Xiaojuan Feng,
Institute of Botany (CAS), China

Reviewed by:
Wei-dong Zhai,
Shandong University, China
Shan Jiang,
East China Normal University, China

***Correspondence:**
Hon-Kit Lui
hklui@mail.nsysu.edu.tw
Chen-Tung Arthur Chen
ctchen@mail.nsysu.edu.tw

Specialty section:
This article was submitted to Biogeoscience, a section of the journal Frontiers in Earth Science

Received: *21 April 2021*
Accepted: *23 August 2021*
Published: *09 September 2021*

Citation:
Lui H-K, Liu M-Y, Lin H-C, Tseng H-C, Liu L-L, Wang F-Y, Hou W-P, Chang R and Chen C-TA (2021) Hydrogeochemistry and Acidic Property of Submarine Groundwater Discharge Around Two Coral Islands in the Northern South China Sea. Front. Earth Sci. 9:697388. doi: 10.3389/feart.2021.697388

Submarine groundwater discharge (SGD) is an important source of nutrients in many coastal regions, yet little information is available on its carbonate chemistry and controlling factors. This study examined the processes and factors controlling the hydrogeochemistry and acidic property of the groundwaters and SGD waters of two isolated coral islands, Liuqiu Island (13 km off southwestern Taiwan) and Dongsha Island (located in the northern South China Sea, 420 km away from Liuqiu Island). Our results showed that the total alkalinity and dissolved inorganic carbon (DIC) of the fresh SGD waters were controlled mainly by the chemical weathering of carbonate minerals. Part of the DIC came from the organic matter decomposition or soil CO_2, reducing the pH and CO_3^{2-} concentration. Distributions of the carbonate chemistry and nutrients of the SGD waters were controlled mainly by physical mixing between the groundwater and the ambient seawater under the seabed, the so-called subterranean estuary. The Ca^{2+} released through weathering significantly increased the saturation state of aragonite or calcite, reducing the corrosiveness of the SGD waters on the carbonate rocks. This study is likely the first to examine the effects of the acidic property of SGD waters on the biogenic carbonate spine of a sea urchin and a pteropod shell. The spring water with similar carbonate chemistry to that of the freshwater SGD endmember from Liuqiu Island with a saturation state of aragonite of 0.96 caused observable dissolution on the spine of a sea urchin and a pteropod shell, but the spine dissolved more readily. This was because the spine is made of high-Mg calcite, which has higher solubility than that of aragonite or calcite. Such a result implies that some marine organisms with carbonate skeletons or shells containing high Mg: Ca ratios may suffer the impact of ocean acidification earlier. Although the SGD may contribute less than 10% of freshwater discharge by rivers to the coastal area, its impact on coastal biogeochemical cycles and ecosystems due to its acidic property and continual effect on the coast all year round deserves further investigation.

Keywords: Dongsha, Liuqiu, ocean acidifcation, pH, saturation state of CaCO, chemical weathering, geochemistry, SGD

INTRODUCTION

River inputs play an essential role in global water cycles and biogeochemical cycles. They transport water and large amounts of nutrients, such as nitrate, phosphate, and silicate, to support the estuaries' high productivity and biodiversity. In addition to the river waters, there is also fresh groundwater discharging into the ocean through the seabed directly. This phenomenon is called submarine groundwater discharge (SGD) (Burnett et al., 2003; Bishop et al., 2017; Taniguchi et al., 2019). Taniguchi et al. (2019) defined SGD as "the flow of water through continental and insular margins from the seabed to the coastal ocean, regardless of fluid composition or driving force", stating that islands typically have higher SGD, in terms of fluxes per unit area of landmass, than continents. According to this definition, the SGD includes both the freshwater and recirculated (or recharged) seawater.

Primarily due to difficulties in observations and measurements, there are not as many studies on SGD as there are on riverine systems. The amount of water fluxes of SGD is considerably high, accounting for 1–10% of the total riverine discharge (Burnett et al., 2001; Santos et al., 2021). However, the proportion of the nutrient flux of the SGD could be higher. This is because SGD water generally has a longer residual time than that of river water before entering the oceans, accumulating a more significant effect of organic matter decomposition; chemical weathering; and human activities, such as sewage inputs and fertilizer leakage. (Wang et al., 2018; Chen et al., 2019; Santos et al., 2021). Consequently, SGD water is usually high in nutrients but low in dissolved oxygen (DO) and pH (Wang et al., 2018). Coupling with the dissolution of minerals, such as $CaCO_3$, SGD water could also be high in dissolved inorganic carbon (DIC) and total alkalinity (TA) (Wang et al., 2018). Since the pre-industrial period, the oceans have been absorbing an increasing amount of human-released CO_2 from the atmosphere. Consequently, the pH, saturation state of calcite (Ω_{Cal}), and aragonite (Ω_{Ara}) are gradually decreasing with time. Such a process is called ocean acidification. Generally speaking, the pH of the surface ocean is around 8.25 on the NBS scale (or about 8.1 on the total scale), and the value is expected to have a 0.3 pH unit drop at the end of this century due to the increasing atmospheric CO_2 (Orr et al., 2005; Hoegh-Guldberg et al., 2007; Dore et al., 2009; Bates et al., 2014). It is well known that ocean acidification reduces the calcification rates of many marine organisms that use $CaCO_3$ as their skeleton. Indeed, SGD could be an acidity source for coastal oceans.

Previous studies have shown that the SGD is a vital source of nutrients in many coastal regions, but little information is available on its carbonate chemistry and the controlling factors. Using Taiwan as an example, a previous study showed that in the coastal region, there is a larger amount of inorganic carbon (such as carbon dioxide) brought in by the SGD than organic carbon produced by phytoplankton from the nutrients brought in by the SGD (Wang et al., 2018). The extra-inorganic carbon may eventually move to the atmosphere in the form of CO_2. That is, SGD is a source of CO_2 that ends up in the atmosphere. Studies have pointed out that the lower the Ω_{Cal} or Ω_{Ara} values, the lower the calcification rate of some marine organisms with calcium carbonate shells (Hoegh-Guldberg et al., 2007). Of note is that the Ω_{Cal} and Ω_{Ara} of SGD water could be lower than one (undersaturation) (Wang et al., 2018). In that case, $CaCO_3$ starts to dissolve. The Ω_{ara} value of the discharged submarine groundwater is anticipated to decrease from oversaturation to undersaturation with the increasing atmospheric CO_2 in Sanya Bay in the northern South China Sea (Wang et al., 2014). Understanding the hydrogeochemistry and carbonate chemistry of the SGD water is critical for examining and predicting the impact of human activities on the chemistry of SGD and on the coastal ecosystem, especially on coral reefs where the highest marine biodiversity exists.

This study aims to investigate the processes and factors controlling the hydrogeochemistry and the acidic property of the SGD water and groundwater of two isolated coral islands, Liuqiu Island (13 km off southwestern Taiwan) and Dongsha Island (located in the northern South China Sea, 420 km away from Liuqiu Island) (**Figure 1**). Liuqiu Island is a 4 km long and 2 km wide NW–SE elongated coral-reef island with an area of 6.8 km^2. The island has been raised at a rate of about 2 mm/year, mainly due to mud diapirism (Shih et al., 1991; Chen et al., 2014). Dongsha Island is a 2.8 km long and 0.9 km wide E–W coral reef island with an area of 1.8 km^2. It is the only reef island among a circular coral reef with a diameter of about 25 km, namely, the Dongsha Atoll. We collected water samples around Liuqiu Island and Dongsha Island. The carbonate chemistry and major ions of rainwaters, spring waters, and SGD waters were analyzed. Factors controlling the chemical weathering and the carbonate chemistry are discussed. This study is likely the first to examine the effect of the acidic property of SGD water on the biogenic carbonate spine of a sea urchin and a pteropod shell.

METHODS AND MATERIALS

Eight expeditions took place on 1987/9/26, 2017/7/13, 2017/9/25, 2019/12/11-13, 2020/6/15-19, 2020/9/17, 2020/12/3, and 2021/1/25 in Liuqiu Island. Four spring waters (S1-S4, **Figure 1B**) were sampled on 1987/9/26, and only the major ions were used in this study. For the remaining seven expeditions between 2017 and 2021, we regularly sampled the spring water (S5, **Figures 1B,C**) as well as the SGD waters and seawaters at the southern tip of Liuqiu Island (station A1, **Figure 1B**). Three expeditions took place on 2020/9/2, 2021/1/5, and 2021/1/11 in Dongsha Island (**Figure 1D**). Two groundwater samples were taken from two wells on 2020/9/2. Groundwater, SGD, and seawater samples were sampled around Dongsha Island on 2021/1/5. A groundwater sample was taken from a well, and two seawater samples were taken from the inner lagoon on 2021/1/11. Fifteen rainwater samples were sampled from two stations (R1 and R2) located in southwestern Taiwan (32 km away from Liuqiu Island) in 2020 on 4/6, 5/19, 5/20, 5/21 (two samples), 5/22 (three samples), 5/27 (two samples), 6/7, 7/15, 8/3, 8/4, and 8/26 (**Figure 1A**).

A hollow stainless steel needle with a total length of 0.5 m was inserted from the water into the seabed 0.2–1 m below the sea surface around the coasts of Liuqiu Island and Dongsha Island. The SGD waters were drawn using the needle and stored immediately in a plastic-made sampling bag to minimize the

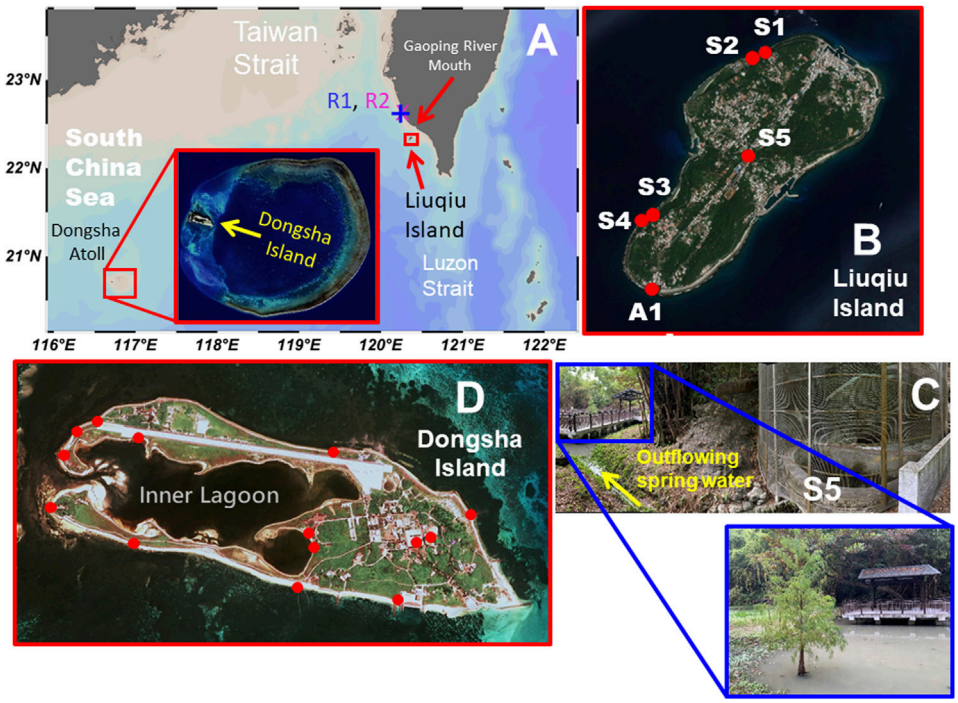

FIGURE 1 | (A) Study areas and sampling locations of **(B,C)** Liuqiu Island and **(D)** Dongsha Island. The satellite image of Dongsha Atoll was taken from the National Geospatial-Intelligence Agency of the U.S. The maps were generated using Ocean Data View 5.0.0. Schlitzer, R., Ocean Data View, https://odv.awi.de, 2018.

gases exchange between the water samples and air. Field water temperature, salinity (or conductivity), and DO were measured using a Hach HQ40 portable multimeter. DO was calibrated using H_2O-saturated air, and salinity was calibrated with the OSIL-produced International Association for the Physical Sciences of the Oceans (IAPSO) salinity standard seawater. Water samples were collected and poisoned with 0.05% saturated $HgCl_2$. Waters for pH, TA, DIC, and CH_4 measurements were stored in borosilicate glass bottles. Waters for nutrient measurements were filtered with a 0.45 μm Millex-HA syringe filter (MF-Millipore mixed cellulose ester membrane) and stored in PP bottles. TA was measured by Gran titration with an open-cell system using the Apollo-manufactured total alkalinity titrator (model: AS-ALK2). DIC was measured with an infrared detector using an Apollo-manufactured DIC analyzer (model AS-C6L). Both TA and DIC were calibrated against certified reference material for ocean CO_2 measurements provided by Dr. A.G. Dickson at the Scripps Institution of Oceanography Marine Physical Laboratory, University of California, San Diego. For the brackish water and seawater samples, pH on the total scale was measured using a spectrophotometer with meta-cresol purple at 25°C. For the freshwater samples, the pH on the NBS scale was measured with a glass electrode pH meter at 25°C. To compare the pH data on the same scale, we converted the pH on the total scale to the NBS scale. The differences in pH values of our samples between two scales (pH on the NBS minus pH on the total scale), determined using the CO_2 System Calculations Program version 2.3 (Pierrot et al., 2006), is as high as 0.16 at a salinity of 1.4 and as low as 0.14 at a salinity of 36.4. pH values reported in this study are on the NBS scale at 25°C.

Two SGD samples collected from Dongsha Island formed black precipitation when $HgCl_2$ was added for preservation. This could be due to the formation of HgS when $HgCl_2$ reacted with the H_2S, which is one of the gases that commonly exist in groundwater. The chemical reaction is as follows:

$$H_2S_{(aq)} + HgCl_{2\ (aq)} \rightarrow HgS_{(s)} + 2HCl_{(aq)}$$

Of note is that this reaction generates hydrochloric acid, further reducing the pH and TA of the water samples. Assuming all the black precipitation was HgS, using its weight, we corrected the changes in TA and pH due to the formation of HCl.

Nitrate plus nitrite, phosphate, and silicate were calibrated with the OSIL nutrient standards, and detailed information was given by Chen and Wang (2006). CH_4 was measured with the head-space equilibration technique (Weiss, 1981) using a gas chromatograph (Agilent 7,890) fitted with a flame ionization detector (FID). The primary standard was 1.16 ppmV CH_4 (MESA Specialty Gas, United States). The precision of repeated analysis of water samples was about ±3% in routine sample analysis. The CO_3^{2-}, HCO_3^-, and partial pressure of CO_2 (pCO_2) were calculated using the CO_2 System Calculations Program version 2.3 (Pierrot et al., 2006). The dissociation constants for the carbonate chemistry were taken from Millero (2010). Ω_{Cal} and Ω_{Ara} were calculated using the following equation:

$$\frac{[Ca^{2+}][CO_3^{2-}]}{K_{sp}}$$

TABLE 1 | Conductivity, salinity, and the major ions of the spring waters at stations S1–S5 and the rainwater at station R1.

Stn	Con	S	Na^+	K^+	Ca^{2+}	Mg^{2+}	Cl^-	SO_4^{2-}	HCO_3^-	Cation	Anion
	μS/m		μmol/kg							μequivalent/kg	
						1987/9/26					
S1	504	0.2	931	40	1,626	152	906	360	2,828	4,528	4,454
S2	656	0.3	877	54	2,438	161	822	350	4,784	6,130	6,307
S3	1,193	0.6	4,102	72	3,168	383	3,915	948	4,448	11,278	10,260
S4	990	0.5	2,366	89	2,925	312	1,659	412	4,554	8,930	7,037
S4	981	0.5	2,366	89	2,925	321	1,639	416	4,551	8,947	7,021
						2020/12/3					
S5	848	0.4	2,194	62	1931	507	1,346	347	6,687	7,133	8,750
						2020/8/26					
R1	2.6	0.0	5.3	0.7	2.3	0.9	4.9	1.4	1.9	12.4	10.2

where K_{sp}, the stoichiometric solubility product, was taken from Mucci (1983).

Major ions were analyzed for the spring waters collected at stations S1–S4 on 1987/9/26, the spring water collected at station S5 on 2020/12/3, and the rainwater collected at R1 on 2020/8/26. Cations of samples collected in 1987 were measured using the Dionex ion chromatography system (model: 2000i). Cl^- was determined using the mercury thiocyanate method (Florence and Farrar, 1971), SO_4^{2-} was determined using turbidimetric method (American Public Health Association, 1981), and HCO_3^- was calculated using the measured TA and pH. Major ions of water samples collected in 2020 were analyzed using ion chromatography at the Ultra Trace Industrial Safety Hygiene Laboratory of the SGS Taiwan Ltd. The results are shown in **Table 1**. For the remaining water samples, the Ca^{2+} used to calculated the Ω_{Cal} and Ω_{Ara} values was estimated using the linear correlation with the spring water at S5 (Ca^{2+} = 1931 μmol/kg at a salinity of 0.42; see **Table 1**) mixed with the standard seawater (Ca^{2+} = 10,282 μmol/kg at a salinity of 35 (Millero et al., 2008)) as endmembers.

A sea urchin, *Hemicentrotus pulcherrimus,* was collected from Liuqiu Island. A 10% KOH solution was used for tissue digestion. The shell of a pteropod, *Creseis virgula,* was collected around the coast of southwestern Taiwan. Spring water collected at station S5 on 2021/12/3, and surface seawater collected at the coast of southwest Taiwan on 2021/1/12 were poisoned with 0.05% saturated $HgCl_2$ and sealed for the incubation experiments. The spine and shell were incubated in a 250 ml borosilicate glass bottle filled with the spring water for 60 days at 25°C. The seawater incubated with the spine was used as the control. On the 30th day, we refreshed the spring water and seawater, as well as taking images under a microscope (model: MSHOT MZ88) using a Canon EOS 600D digital camera on the 1st, 30th and 60th days.

RESULTS AND DISCUSSION

Major Ions and Their Implied Material Source From Chemical Weathering

Table 1 shows the conductivity, salinity, and the major ions of the spring waters at stations S1–S5 and the rainwater at station R1. Generally speaking, atmospheric depositions and the chemical weathering of rocks are two significant sources of ions for natural waters. Human activities, such as sewage input, could also contribute major ions. Of note is that the low CH_4 concentrations of the spring water (**Table 2**) suggested that the influence of human activities on the major ions of the spring water was minimal, as local sewage discharge usually has several orders of magnitude higher in CH_4 concentration (Borges et al., 2018). Major ions in the spring waters of Liuqiu Island are contributed mainly from the chemical weathering of rocks, as the major cations (Na^+, K^+, Ca^{2+}, Mg^{2+}) and anions (Cl^-, SO_4^{2-}, HCO_3^-) in rainwater collected on 2020/8/26 were negligibly small when compared with the spring water in Liuqiu Island collected on 2020/12/3 (**Table 1**). Taking Na^+, K^+, Ca^{2+}, Mg^{2+} as examples, the rainwater was able to contribute only 0.2, 1.1, 0.1, and 0.2%, respectively, to that of the spring water. Such a result implies that various chemical weathering processes contribute the most to the spring water's major ions. The positive correlations between the major ions and salinity of the spring waters of Liuqiu Island and the rainwater provided further evidence for this suggestion (**Figure 2**). Several chemical weathering reactions are listed as follows:

The dissolution of halite:

$$NaCl \rightarrow Na^+ + Cl^- \quad (1)$$

The dissolution of a silicate mineral (using sodium feldspar as an example):

$$2NaAlSi_3O_8 + 2H_2CO_3 + 9H_2O \rightarrow 2Na^{2+} + 2HCO_3^- + 4H_4SiO_4 + Al_2Si_2O_5(OH)_4 \quad (2)$$

The dissolution of $CaCO_3$ or $MgCO_3$ (using $CaCO_3$ as an example):

$$CaCO_3 + H_2CO_3 \rightarrow Ca^{2+} + 2HCO_3^- \quad (3)$$

The dissolution of dolomite:

$$Mg_{(1-x)}Ca_xCO_3 + CO_2 + H_2O \rightarrow (1-x)Mg + xCa^{2+} + 2HCO_3^- \text{ and } (0 \leq x \leq < 1) \quad (4)$$

The oxidation of pyrite:

TABLE 2 | Flow rate, temperature, salinity, DO, pH on the NBS scale, DIC, TA, CO_3^{2-}, pCO_2, $NO_3^- + NO_2^-$, PO_4^{3-}, SiO_2, CH_4, Ca^{2+}, Ω_{Ara}, and the Ω_{Cal} of the spring water at S5 on Liuqiu Island between 2017 and 2021.

Date	Spring water in liuqiu island															
	Flow rate	Temp	S	DO	pH	DIC	TA	CO_3^{2-a}	pCO_2^a	$NO_3^- + NO_2^-$	PO_4^-	SiO_2	CH_4	Ca^{2+a}	Ω_{Ara}^a	Ω_{Cal}^a
	L/s	°C		mg/L			μmol/kg		(μatm)		μM		nM	μmol/kg		
2017/7/13	—	27.3	0.45	5.31	—	7,931	—	—	—	122.0	—	239.4	—	1939	—	—
2019/12/12	0.42	26.7	0.41	5.54	—	7,569	6,624	7.80	29,448	156.0	0.88	234.1	37.3	1929	1.13	1.85
2020/6/15	1.40	27.1	0.41	5.22	7.21	7,819	6,630	6.26	37,316	163.2	1.32	227.5	13.9	1929	0.92	1.50
2020/6/19	—	27.0	0.41	5.25	7.25	7,376	—	—	—	—	—	—	—	1929	—	—
2020/9/17	—	28.1	0.40	5.39	7.15	7,309	6,539	9.36	24,988	152.2	1.19	224.4	15.2	1926	1.40	2.28
2020/12/3	0.74	27.0	0.42	5.12	7.02	7,848	6,701	6.66	35,930	100.0	1.31	230.0	7.8	1931[b]	0.96	1.57
2021/1/25	0.18	25.6	0.43	5.90	7.13	7,692	6,704	7.64	29,896	89.4	0.81	235.6	—	1934	1.07	1.76
Average	0.69 ±0.53	27.0 ±0.8	0.42 ±0.02	5.39 ±0.26	7.15 ±0.09	7,649 ±240	6,640 ±68	7.55 ±1.2	31,514 ±5,062	130.5 ±31.3	1.10 ±0.24	230.8 ±5.3	18.6 ±12.9	1931 ±4.05	1.10 ±0.19	1.79 ±0.31

[a]*Calculated (see Methods and Materials).*
[b]*direct measurement.*

$$4FeS_2 + 15O_2 + 8H_2O \rightarrow 2Fe_2O_3 + 8H_2SO_4 \quad (5)$$

Na^+ was the most or second most abundant among the cations, followed by Ca^{2+} in the rainwater and spring waters, whereas HCO_3^- was the most abundant anion followed by Cl^- (**Table 1**). Generally, Cl^- ion mainly came from halite dissolution or marine spacy. Seawater has a Na^+: Cl^- ratio of approximately 0.86 (Millero et al., 2008). In contrast, the freshwater samples shown in **Table 1** had excess Na^+ rather than Cl^- with ratios between 1.03 and 1.63. The almost 1:1 correlation between the Na and Cl ions (**Figure 3**) suggested that the Cl^- and the equivalent of Na^+ came from the halite dissolution or marine spacy. The remaining Na^+ (Na^+ minus Cl^-, corrected for halite dissolution contribution) and K^+ were from Na- or K-feldspar weathering, which was expected to contribute the same amount of TA in the form of bicarbonate ion as shown in **Eq. 2**. Such a result is in accordance with previous study that in Liuqiu Island siliceous soils cover carbonate rocks (Holocene coral reef or Pleistocene limestone) (Cheng et al., 2011). The carbonate rocks' dissolution mainly contributes to the Ca^{2+} and Mg^{2+} ions (see **Eqs 3, 4**. The $[Ca^{2+}]/[Mg^{2+}]$ ratio of 3.8 of the spring water is in accordance with that of the soil pedons in Liuqiu Island, ranging between 1.4 and 7.1 (average 3.7 ± 1.9, n = 21) (Cheng et al., 2011). The SO_4^{2-} could be contributed by the $CaCO_3$ or $MgCO_3$ dissolution with the participation of H_2SO_4 instead of H_2CO_3. But this is unlikely to explain the amount of SO_4 found in the spring waters of Liuqiu Island, as the rainwater contained a negligibly small amount of SO_4. Pyrite oxidation (see **Eq. 5**) might contribute the SO_4 to the spring water and the surface freshwaters in Liuqiu Island. Under pyrite oxidation, 1 mol of SO_4 formation would lead to 2 mol of TA deduction due to sulfuric acid formation.

Carbonate Chemistry and the Acidic Property of Spring Water

Rainwaters sampled contained only a small amount of TA (-19–94 μmol/kg, n = 9) and DIC 38–89 μmol/kg, n = 9), whereas our time-series data at station S5 showed that the spring water at S5 had significantly higher TA (6,624–6,704 μmol/kg) and DIC (7,309–7,931 μmol/kg) values (**Table 2**). As mentioned above, the dissolution of feldspar or carbonate rocks contributed TA and DIC. Based on **Eqs 1–3**, regarding the spring water sampled on 2020/12/3, we estimated $(Na^+ - Cl^-) + K^+ + 2(Ca^{2+} + Mg^{2+}) = 5787$ μmol/kg for TA and $(Ca^{2+} + Mg^{2+}) = 2439$ for DIC. Note that $CaCO_3$ or $MgCO_3$ weathering consumed CO_2. The organic matter decomposition could contribute to this CO_2 in the groundwater. Soil air has a significantly higher CO_2 concentration than that of the atmosphere and could also contribute to the CO_2 in the groundwater. Using the TA value, we calculated that the DIC value to be 6,252 μmol/kg when the pCO_2 was the same as that in the atmosphere (about 400 μatm; 100% humidity). That is, we estimated that there was (7,848–6,252) = 1,596 μmol/kg of excess DIC or CO_2 in the spring water with respect to the atmospheric CO_2 level. **Figure 4** shows the estimations. Again, this amount of CO_2 could be contributed by the organic matter decomposition or by soil air. Organic matter decomposition increased the DIC value but slightly decreased the TA value. In comparison, the CO_2 gas exchange between soil air and groundwater would not change TA. However, we could not quantify the amount of TA change with this 1,596 μmol/kg excess CO_2, as we could not quantify the amount of CO_2 in the soil air–groundwater CO_2 exchange or in the groundwater's organic matter decomposition. Based on **Eqs 1–3**, we estimated the TA value of the spring water to be 5,787 μmol/kg, explaining 86% of the measured value of 6,701 μmol/kg. The excess CO_2 of 1,596 μmol/kg accounted for 20% of the measured DIC of 7,848 μmol/kg (**Figure 4**). Such results suggest that the chemical weathering mainly contributed to the TA and DIC values, and part of the DIC was contributed by the increase in CO_2 through organic matter decomposition or soil air–groundwater CO_2 exchange.

Surface seawaters around southwest Taiwan and in the northern South China Sea generally had pH values of about 8.20 (about 8.05 on the total scale) or higher (Chen et al., 2010; Lui and Chen, 2015; 2017). In contrast, the spring waters collected between 2017 and 2021 had a relatively low pH value, ranging

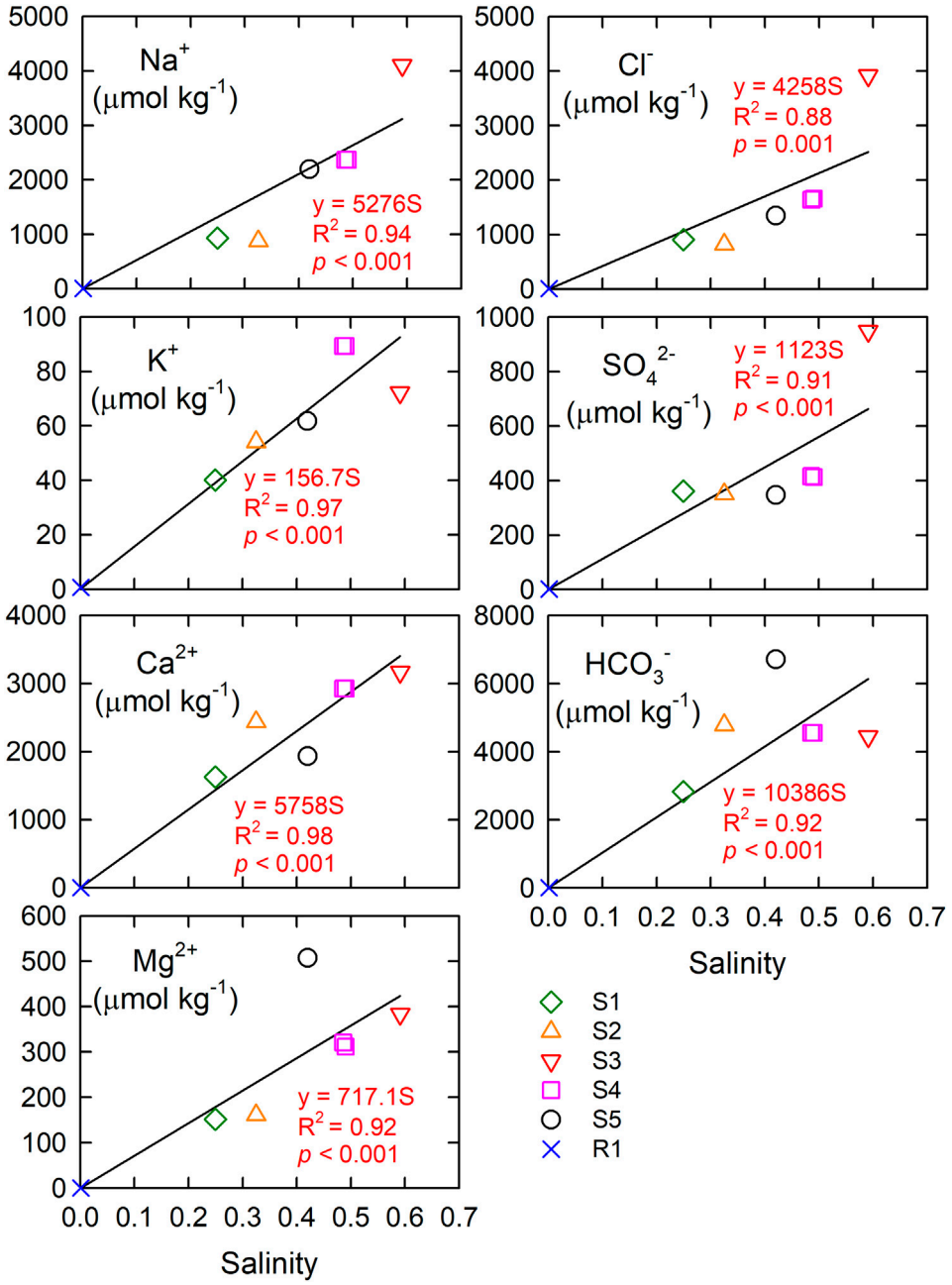

FIGURE 2 | Major ions vs. salinity of the rainwater at R1 and the spring waters at S1–S5 on Liuqiu Island. The solid lines show the linear regression lines passing the origins.

7.02–7.25 and averaging 7.15 ± 0.09 (n = 5). The dissolution of carbonate rock consumes dissolved CO_2 and generates TA and DIC in a ratio of 2:1. Feldspar dissolution consumes CO_2 and generates TA as well. That is, increasing TA and DIC in a ratio equal to or higher than 2:1 increases the pH, Ω_{Ara}, and Ω_{Cal} values but decreases the pCO_2 value. Such a change also increases the carbonate buffering capacity of a water body by reducing the extent by which the pH, Ω_{Ara}, and Ω_{Cal} values are reduced under additional CO_2 dissolution (Chou et al., 2013). Indeed, these water bodies' relatively low pH values were mainly due to the dissolution of CO_2 through the soil air–groundwater CO_2 exchange and organic matter decomposition. Although the dissolution of carbonate rocks generated a considerable amount of CO_3^{2-} and Ca^{2+}, the addition of a high amount of excess CO_2 reduced the CO_3^{2-} concentrations of the spring waters to just 6.3–9.4 μmol/kg due to thermodynamics. Consequently, the Ω_{Ara} and Ω_{Cal} were 0.92–1.40 and 1.50–2.28, respectively. With a considerable amount of excess CO_2, the pCO_2 of the spring waters could be as high as 37,316 μatm (**Table 2**).

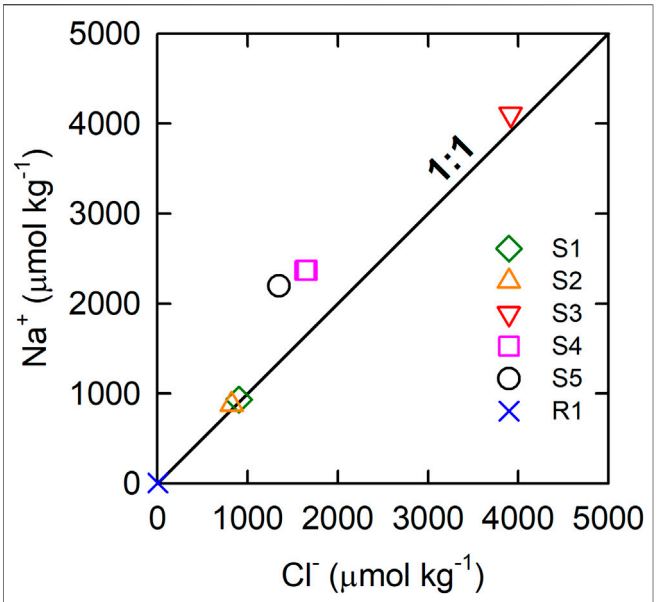

FIGURE 3 | Na^- vs. Cl^- of the rainwater and spring waters on Liuqiu Island. **Table 1** shows the information in detail. The solid line shows the 1:1 ratio.

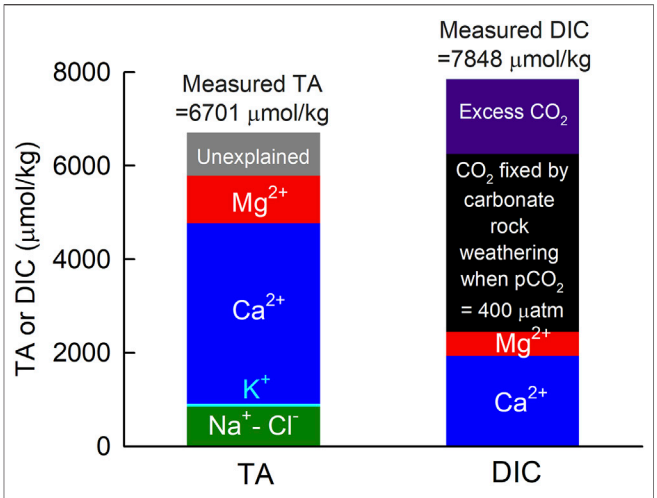

FIGURE 4 | Estimated TA and DIC of the spring water at station S5 using major ion concentrations and the excess CO_2 calculated with measured TA and pCO_2 = 400 μatm, assuming the air–water CO_2 equilibrium.

Physical Mixing Behaviors in the Subterranean Estuaries

In Liuqiu Island, the values of temperature, DO, pH, TA, DIC, Ω_{Ara}, and SiO_2 in the spring water did not considerably change across seasons (**Figure 5**). The temperatures of the SGD samples and seawaters showed strong seasonal variations. The strong negative linearities between TA, DIC, NO_3^- + NO_2^-, SiO_2, and the salinity of the SGD samples suggested that the carbonate chemistry and nutrients of the SGD samples were controlled mainly by physical mixing between the groundwater and ambient seawater within the seabed, the so-called subterranean estuary. The freshwater endmembers of the TA, DIC, and SiO_2, determined using the SGD data and linear regressions methods, were similar to those of the spring water, suggesting that the carbonate chemistry of the discharged submarine groundwater at station A1 had similar carbonate chemistry to that of the spring water at station S5, which had no observable changes across seasons. The differences in TA and DIC between the linear-regression determined freshwater endmembers of the SGD samples and the spring waters were (7,917–6,640) = 1,277 μmol/kg and (8,330–7,649) = 681 μmol/kg, respectively (**Figure 5**; **Table 2**). The differences in TA and DIC had a ratio of 1.88. Such a result reflects that the higher TA and DIC of the SGD freshwater endmembers were mainly due to the further dissolution of carbonate rocks, which has changes of TA and DIC in a ratio of two. Generally, water with a lower pH or Ω_{Ara} value is more corrosive to $CaCO_3$. Although the spring water contained a very low CO_3^{2-} concentration, it had a Ω_{Ara} value that was sometimes slightly below one. This is because the spring water contained a high concentration of Ca^{2+} that came from the weathering of the $CaCO_3$ rock, increasing the Ω_{ara} value. That is, the dissolution of $CaCO_3$ minerals around the coral islands effectively reduced the corrosiveness of the groundwater and hence the SGD water, reducing the environmental stress that was due to the discharge of the acidic SGD. Meanwhile, the linearities of TA and DIC vs. salinity of the SGD samples in Liuqiu Island suggested that the residual time of the groundwater in the freshwater–seawater mixing zones, the so-called subterranean estuaries, was short. The increase in buffering effect of the SGD water due to an additional dissolution of carbonate rock in the subterranean estuary was insignificant, making SGD is an additional acidic source with similar carbonate chemistry of the groundwater for the coastal areas.

The SGD waters likely had a freshwater endmember with a lower NO_3^- concentration than that of the spring water. The PO_4^{3-} was scattered across the salinity gradient largely because the groundwater and the ambient seawater contained similar but low concentrations of PO_4^{3-}. The use of chemical fertilizer could be an important source of nutrients for groundwater. According to the Liuqiu Township Office, only 0.01 km^2 (0.15% of the total area) is farmland in Liuqiu Island. Most important is that nearly all of the farmland is dryland. Without sufficient freshwater (such as river water) to support a considerable scale of agriculture, the influence of the use of fertilizer on the chemistry of the groundwater in Liuqiu Island or Dongsha Island is expected to be insignificant. Sewage input could be another critical factor influencing the chemistry of groundwater in Liuqiu Island or Dongsha Island. In Liuqiu Island, the CH_4 concentrations were low for both the spring water and SGD samples, showing no observable influence of anthropogenic activities in our sampling sites, such as local sewage discharge, which is usually several orders of magnitude higher in CH_4 concentration (Borges et al., 2018). Noting, fresh SGD can be observed in Liuqiu Island in both the wet and dry seasons, showing that it has a continual effect on

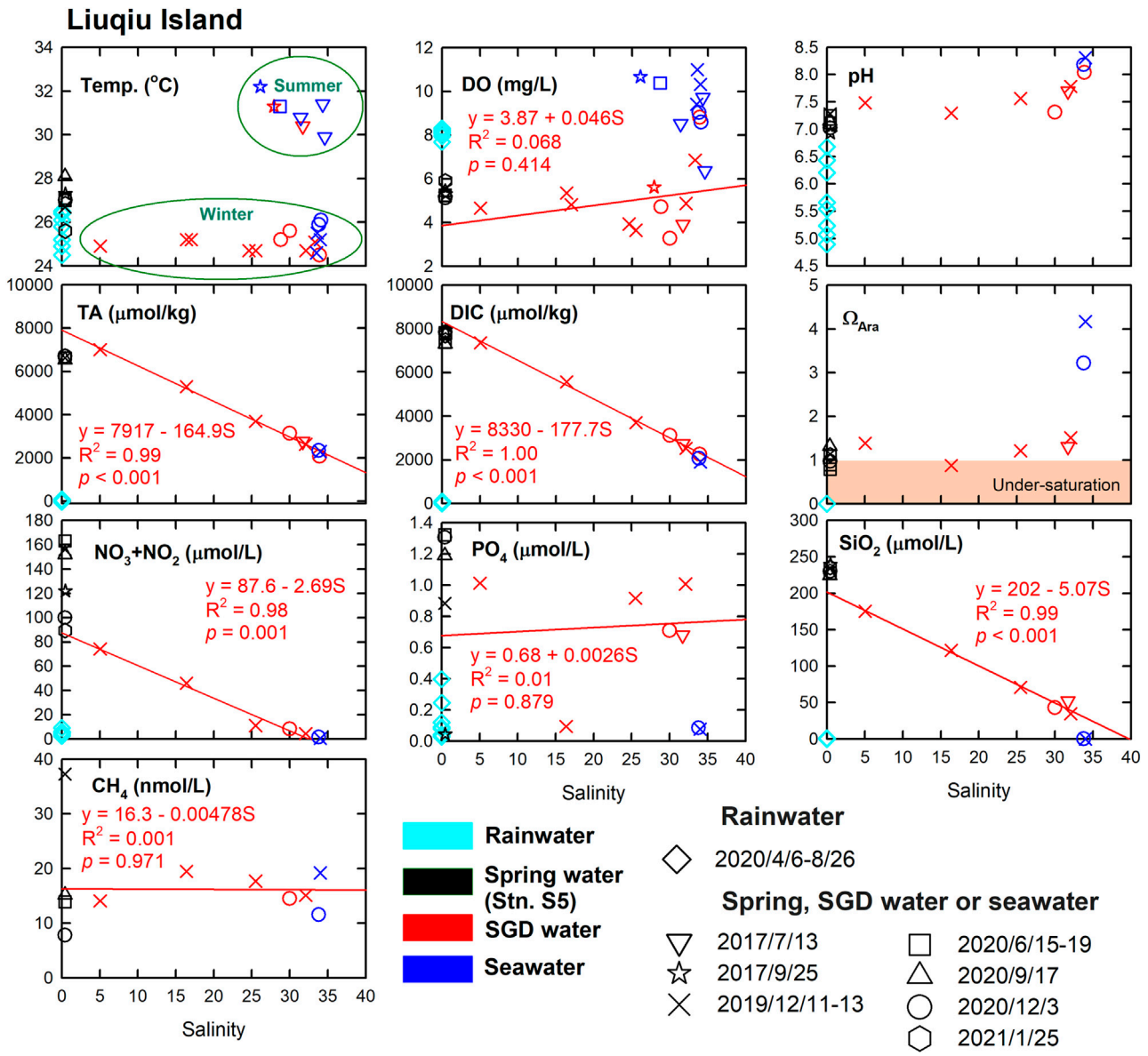

FIGURE 5 | Temperature, DO, pH, TA, DIC, Ω_{Ara}, $NO_3^- + NO_2^-$, PO_4^{3-}, SiO_2, and CH_4 vs. salinity of rainwater, spring water, SGD water, and seawater in Liuqiu Island. The rainwater, spring water, SGD water, and seawater are in light blue, black, red, and blue, respectively. The red lines extended to the axes and equations show the linear regressions for the conservative parameters of the SGD data.

the coast of Liuqiu Island all year round. In contrast, the surface seawaters had high DO, pH, and Ω_{ara} values but low nutrient concentrations. Such a result was likely due to the enhanced productivity achieved *via* the support of nutrients from the SGD or from the Gaoping River, which is about 13 km from Liuqiu Island. Local discharges may also affect this and warrant further investigation.

In Dongsha Island, which is about 420 km from Liuqiu Island, the DO and pH of the groundwater, SGD waters, and seawaters had positive correlations with salinity, whereas the TA, DIC $NO_3^- + NO_2^-$, PO_4^{3-}, SiO_2 and CH_4 showed negative correlations with salinity (**Figure 6**). Such results suggest that the carbonate chemistry and nutrients of the SGD waters were controlled mainly by physical mixing between the groundwater and seawaters. Furthermore, the carbonate chemistry and nutrients of water samples collected over the wet and dry seasons in Dongsha Island were consistent with each other, showing stable chemical properties of the groundwater endmember for the SGD waters. Interestingly, the trends of the pH, TA and DIC vs. salinity plots suggested that the freshwater endmembers of the SGD waters in Dongsha Island were similar to those in Liuqiu Island. Such a result suggests that the factors controlling the carbonate chemistry of the groundwaters and SGD waters in Dongsha Island might be

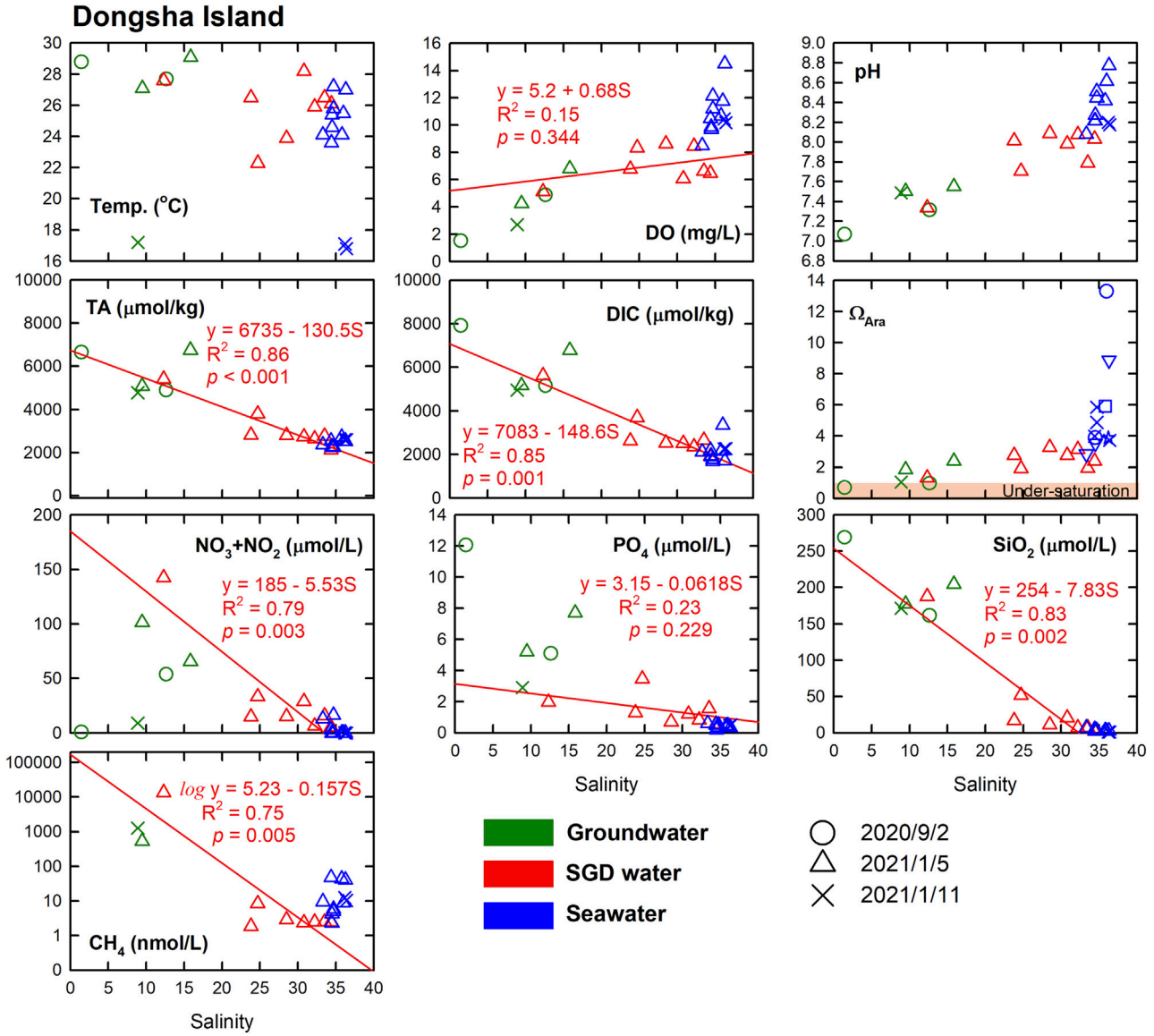

FIGURE 6 | Temperature, DO, pH, TA, DIC, Ω_{Ara}, $NO_3^- + NO_2^-$, PO_4^{3-}, SiO_2, and CH_4 vs. salinity of groundwater, SGD water, and seawater in Dongsha Island. The groundwater, SGD, and seawater are in green, red, and blue, respectively. The red lines extended to the axes and equations show the linear regressions for the conservative parameters of the SGD data.

similar to those in Liuqiu Island. In the seagrass meadows in the inner lagoon, the TA and DIC released from the sediment, as well as the high productivity increased the TA:DIC ratio, making the seawater around the seagrass meadows high in DO, TA, pH and Ω_{Ara} but low in DIC and pCO_2 values (Chou et al., 2018). Our water samples were likely not affected by the seawater with relatively high TA but low DIC from the seagrass meadows, maintaining values similar to that of the offshore surface waters. Notably, in Dongsha Island, the high CH_4 and PO_4^{3-} concentrations of the groundwaters, SGD waters, and seawaters suggest that sewage discharges might have affected these waters. Similar to the case in Liuqiu Island, fresh SGD waters could be found around Dongsha Island in the dry season when the rainfall was low, suggesting that the SGD in Dongsha Island maintains a continual effect around the coast all year round and not to mention in the wet season when the rainfall is high.

Effect of Acidic Property and Corrosiveness of SGD on $CaCO_3$ Skeleton and Shells

Notably, the pH could be as low as 7.02 for the spring water in Liuqiu Island and 7.07 for the groundwater in Dongsha Island (**Figures 5**, **6**). Most pH values of the SGD samples in Liuqiu Island and Dongsha Island, however, were far below 7.95, reaching as low as 7.30 for Liuqiu Island and 7.34 for

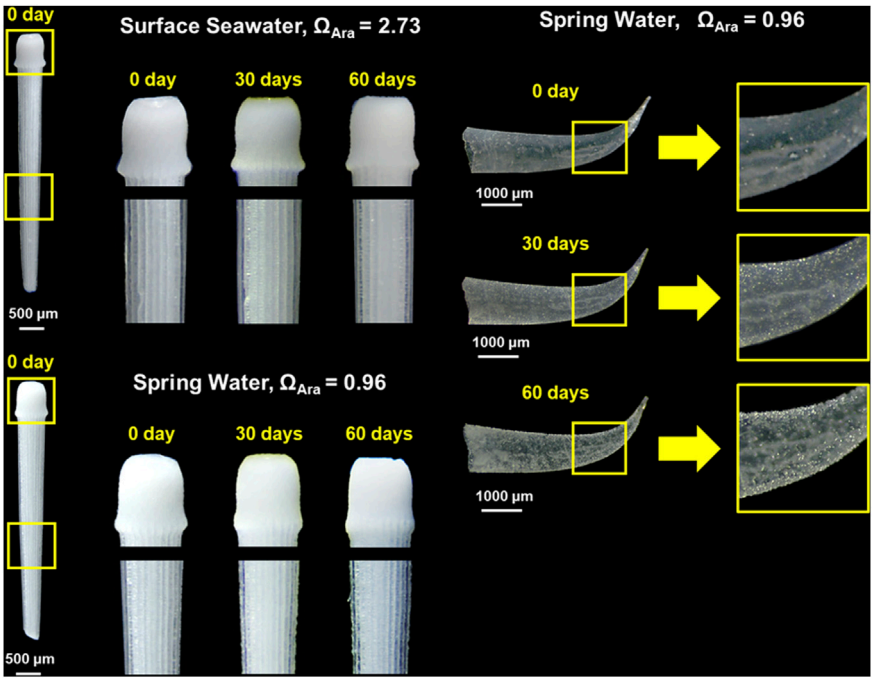

FIGURE 7 | Images of (bottom left) the spine of *H. pulcherrimus* and (right) shell of *C. virgula* before (0 days) and after incubation in the spring water at station S5 with Ω_{Ara} = 0.96 for 30 and 60 days. Seawater with Ω_{Ara} = 2.73 incubated with (top left) the spine of *H. pulcherrimus* was used as the control.

Dongsha Island. Such results reflect the acidic properties of the groundwaters and SGD waters in these two coral reef Islands. As mentioned above, the spring water at station S5 in Liuqiu Island had similar carbonate chemistry to that of the fresh SGD endmembers in Liuqiu and Dongsha Islands. Although the spring water and biogenic carbonate minerals are spatially separated, interactions between the spring water and biogenic carbonate minerals could provide insights into the acidic effects of the SGD on carbonate skeletons and shells. On this basis, the spring water of Liuqiu Island collected on 2020/12/3 with a Ω_{Ara} of 0.96 and preserved with saturated $HgCl_2$ was used to conduct an incubation experiment. A surface seawater sample collected at the coast of southwestern Taiwan on 2021/1/12 with a Ω_{Ara} value of 2.73 was used for comparison. The spines of sea urchins (*H. pulcherrimus*) were incubated in the water samples and observed after 30 and 60 days. The shell of a pteropod (*C. virgula*) was also incubated in the spring water for observation.

The incubation results showed that the spine of *H. pulcherrimus* had no observable difference after incubation in seawater for 60 days (**Figure 7**). In contrast, the spine showed significant dissolution after 30 days and 60 days incubations in the spring water of Liuqiu Island. The base of the spine showed a reduction in size, and the shaft of the spine was etched, becoming rough (**Figure 7**). The shell of *C. virgula* also showed an indication of dissolution, turning from transparent to milky white. Since $HgCl_2$ was added to inhibit microbial activity, we expected that the dissolution of the spine or shell caused by microbial activities to be insignificant. Our observation showed that the spine of the sea urchin dissolved more readily than the shell of the pteropod. This was because the spine of the sea urchin is composed of high-magnesium calcite, which has higher solubility than that of aragonite (Grossmann and Nebelsick, 2013; Haese et al., 2014). Furthermore, even though the shells of pteropods are composed of aragonite, the shapes, microstructures, and $MgCO_3$:$CaCO_3$ ratio of the shells are different, causing the shells to have different solubility and dissolution rates.

It is worth mentioning that our incubation experiments indicated the acidic property of SGD on biogenic carbonate minerals. However, the effects of acidic SGD on live marine organisms are expected to be more complicated. This is because Ω_{Ara} and other factors, such as pH, temperature, pCO_2 and dissolved oxygen, also influence the physiology of marine organisms (Glover and Kidwell, 1993; Shirayama and Thornton, 2005; Kroeker et al., 2013; Van de Waal et al., 2013; Peck et al., 2016; Mekkes et al., 2021). Moreover, the outermost organic layer, periostracum, or other organic matters of many calcifying organisms can effectively counter the $CaCO_3$ dissolution under an acidic environment (Glover and Kidwell, 1993; Peck et al., 2016). Of note is that both incubation experiments and field samples showed that acidified conditions enhanced carbonate shell dissolution and reduced calcification rates of many live calcifying organisms (Glover and Kidwell, 1993; Orr et al., 2005; Shirayama and Thornton, 2005; Hall-Spencer et al., 2008; Talmage and Gobler, 2010; Lischka et al., 2011; Moya et al., 2016; Peck et al., 2016; Zhai, 2018; Li and Zhai, 2019; Zhai et al., 2019; Mekkes et al., 2021). Indeed, the reported acidified conditions

mostly had higher pH and Ω_{ara} values but lower pCO_2 values than that of the SGD samples in Liuqiu Island or Dongsha Island. For instance, the shell of *Limacina helicina* significantly degraded after 29 days of incubation when pH on the total scale and pCO_2 were 7.66 and 1,150 μatm, respectively (Lischka et al., 2011). In the North Yellow Sea, the community net calcification rate was nearly zero when the Ω_{ara} value reached 1.5–1.6 (Zhai, 2018; Li and Zhai, 2019; Zhai et al., 2019). Additionally, the $CaCO_3$ sediments would be dissolved when the Ω_{ara} value of the seawater reached 2.92 ± 0.16 or lower (Eyre et al., 2018). This is largely due to the additional acidic effect as a result of the CO_2 produced by the decomposition of organic matter in sediment. The Liuqiu Island and Dongsha Island examples reveal that SGD could be an important acidic input to coastal oceans.

CONCLUSION

The hydrogeochemistry and carbonate chemistry of the groundwaters, SGD waters, and the seawaters in two coral islands were examined in this study. Our results show that although the dissolution of carbonate rocks increased pH, Ω_{Ara}, Ω_{Cal} and the buffering capacity of the groundwater, the CO_2 from the organic matter decomposition or soil CO_2 enhanced the corrosiveness of the groundwater, shifting Ω_{Ara} from oversaturation to undersaturation. The acidic property of the SGD waters was verified using biogenic carbonate minerals. Although SGD amounts to only several percent of the riverine discharge, it is a common natural phenomenon that could affect the coast all year round, especially in winter when there is minimal rainfall. We suggest that the impacts of SGD on coastal biogeochemical cycles and ecosystems due to its acidic property and continual effect on the coast all year round deserve consideration in further investigations.

DATA AVAILABILITY STATEMENT

The raw data supporting the conclusion of this article will be made available by the authors.

AUTHOR CONTRIBUTIONS

H-KL designed and led the writing of the manuscript. C-TAC was responsible for the overall structure of the manuscript. H-KL, M-YL, F-YW, and RC participated in the sampling. H-KL, RC, H-CT, and W-PH participated in the measurements. H-CL provided the pteropod samples and assisted in taking images. H-CL and L-LL provided advice for the incubation experiment. All authors read and commented on the final version of the manuscript.

FUNDING

This research was funded by the Ministry of Science and Technology of Taiwan (MOST 107-2611-M-110-026-, MOST 108-2611-M-110-025, MOST 109-2611-M-110-010, MOST 109-2611-M-110-016, MOST 110-2611-M-110-024).

ACKNOWLEDGMENTS

Chih-Chieh Su, Feng-Sin Hsu, Pei-Fen Chen, Ting-Hsuan Huang, Sheng-Xiang Xu, and research assistants from Dongsha Atoll Research Station are acknowledged for their assistance during sampling in Dongsha Island. Three reviewers provided detailed and constructive comments, which helped strengthen the manuscript.

REFERENCES

American Public Health Association (1981). *Standard Methods for the Examination of Water and Wastewater*. Wigtown, United Kingdom: American Public Health Association.

Bates, N., Astor, Y., Church, M., Currie, K., Dore, J., Gonaález-Dávila, M., et al. (2014). A Time-Series View of Changing Ocean Chemistry Due to Ocean Uptake of Anthropogenic CO_2 and Ocean Acidification. *Oceanog* 27 (1), 126–141. doi:10.5670/oceanog.2014.16

Bishop, J. M., Glenn, C. R., Amato, D. W., and Dulai, H. (2017). Effect of Land Use and Groundwater Flow Path on Submarine Groundwater Discharge Nutrient Flux. *J. Hydrol. Reg. Stud.* 11, 194–218. doi:10.1016/j.ejrh.2015.10.008

Borges, A. V., Darchambeau, F., Lambert, T., Bouillon, S., Morana, C., Brouyère, S., et al. (2018). Effects of Agricultural Land Use on Fluvial Carbon Dioxide, Methane and Nitrous Oxide Concentrations in a Large European River, the Meuse (Belgium). *Sci. Total Environ.* 610-611, 342–355. doi:10.1016/j.scitotenv.2017.08.047

Burnett, W. C., Bokuniewicz, H., Huettel, M., Moore, W. S., and Taniguchi, M. (2003). Groundwater and Pore Water Inputs to the Coastal Zone. *Biogeochemistry* 66 (1), 3–33. doi:10.1023/B:BIOG.0000006066.21240.53

Burnett, W. C., Taniguchi, M., and Oberdorfer, J. (2001). Measurement and Significance of the Direct Discharge of Groundwater into the Coastal Zone. *J. Sea Res.* 46 (2), 109–116. doi:10.1016/S1385-1101(01)00075-2

Chen, C.-T. A., Huang, T. H., Lui, H. K., and Zhang, J. (2019). Unheralded Submarine Groundwater Discharge. *Ofoaj* 10 (5), 555797. doi:10.19080/ofoaj.2019.10.555797

Chen, C.-T. A., and Wang, S.-L. (2006). A Salinity Front in the Southern East China Sea Separating the Chinese Coastal and Taiwan Strait Waters from Kuroshio Waters. *Continental Shelf Res.* 26 (14), 1636–1653. doi:10.1016/j.csr.2006.05.003

Chen, C.-T. A., Jan, S., Huang, T.-H., and Tseng, Y.-H. (2010). Spring of No Kuroshio Intrusion in the Southern Taiwan Strait. *J. Geophys. Res.* 115 (C8). doi:10.1029/2009jc005804

Chen, S.-C., Hsu, S.-K., Wang, Y., Chung, S.-H., Chen, P.-C., Tsai, C.-H., et al. (2014). Distribution and Characters of the Mud Diapirs and Mud Volcanoes off Southwest Taiwan. *J. Asian Earth Sci.* 92, 201–214. doi:10.1016/j.jseaes.2013.10.009

Cheng, C.-H., Jien, S.-H., Tsai, H., and Hseu, Z.-Y. (2011). Geomorphological and Paleoclimatic Implications of Soil Development from Siliceous Materials on the Coral-Reef Terraces of Liuchiu Island in Southern Taiwan. *Soil Sci. Plant Nutr.* 57 (1), 114–127. doi:10.1080/00380768.2010.548308

Chou, W.-C., Chu, H.-C., Chen, Y.-H., Syu, R.-W., Hung, C.-C., and Soong, K. (2018). Short-term Variability of Carbon Chemistry in Two Contrasting Seagrass Meadows at Dongsha Island: Implications for pH Buffering and CO_2 Sequestration. *Estuarine, Coastal Shelf Sci.* 210, 36–44. doi:10.1016/j.ecss.2018.06.006

Chou, W.-C., Gong, G.-C., Hung, C.-C., and Wu, Y.-H. (2013). Carbonate Mineral Saturation States in the East China Sea: Present Conditions and Future Scenarios. *Biogeosciences* 10 (10), 6453–6467. doi:10.5194/bg-10-6453-2013

Dore, J. E., Lukas, R., Sadler, D. W., Church, M. J., and Karl, D. M. (2009). Physical and Biogeochemical Modulation of Ocean Acidification in the Central North Pacific. *Proc. Natl. Acad. Sci.* 106 (30), 12235–12240. doi:10.1073/pnas.0906044106

Eyre, B. D., Cyronak, T., Drupp, P., De Carlo, E. H., Sachs, J. P., and Andersson, A. J. (2018). Coral Reefs Will Transition to Net Dissolving Before End of Century. *Science* 359 (6378), 908–911. doi:10.1126/science.aao1118

Florence, T. M., and Farrar, Y. J. (1971). Spectrophotometric Determination of Chloride at the Parts-Per-Billion Level by the Mercury(II) Thiocyanate Method. *Analytica Chim. Acta* 54 (2), 373–377. doi:10.1016/s0003-2670(01)82142-5

Glover, C. P., and Kidwell, S. M. (1993). Influence of Organic Matrix on the Post-mortem Destruction of Molluscan Shells. *J. Geology.* 101 (6), 729–747. doi:10.1086/648271

Grossmann, J. N., and Nebelsick, J. H. (2013). Comparative Morphological and Structural Analysis of Selected Cidaroid and Camarodont Sea Urchin Spines. *Zoomorphology* 132 (3), 301–315. doi:10.1007/s00435-013-0192-5

Haese, R. R., Smith, J., Weber, R., and Trafford, J. (2014). High-magnesium Calcite Dissolution in Tropical continental Shelf Sediments Controlled by Ocean Acidification. *Environ. Sci. Technol.* 48 (15), 8522–8528. doi:10.1021/es501564q

Hall-Spencer, J. M., Rodolfo-Metalpa, R., Martin, S., Ransome, E., Fine, M., Turner, S. M., et al. (2008). Volcanic Carbon Dioxide Vents Show Ecosystem Effects of Ocean Acidification. *Nature* 454 (7200), 96–99. doi:10.1038/nature07051

Hoegh-Guldberg, O., Mumby, P. J., Hooten, A. J., Steneck, R. S., Greenfield, P., Gomez, E., et al. (2007). Coral Reefs under Rapid Climate Change and Ocean Acidification. *Science* 318 (5857), 1737–1742. doi:10.1126/science.1152509

Kroeker, K. J., Kordas, R. L., Crim, R., Hendriks, I. E., Ramajo, L., Singh, G. S., et al. (2013). Impacts of Ocean Acidification on Marine Organisms: Quantifying Sensitivities and Interaction with Warming. *Glob. Change Biol.* 19 (6), 1884–1896. doi:10.1111/gcb.12179

Li, C.-L., and Zhai, W.-D. (2019). Decomposing Monthly Declines in Subsurface-Water pH and Aragonite Saturation State from Spring to Autumn in the North Yellow Sea. *Continental Shelf Res.* 185, 37–50. doi:10.1016/j.csr.2018.11.003

Lischka, S., Büdenbender, J., Boxhammer, T., and Riebesell, U. (2011). Impact of Ocean Acidification and Elevated Temperatures on Early Juveniles of the Polar Shelled Pteropod Limacina Helicina: Mortality, Shell Degradation, and Shell Growth. *Biogeosciences* 8 (4), 919–932. doi:10.5194/bg-8-919-2011

Lui, H.-K., and Arthur Chen, C.-T. (2015). Deducing Acidification Rates Based on Short-Term Time Series. *Sci. Rep.* 5 (1), 11517. doi:10.1038/srep11517

Lui, H.-K., and Chen, C.-T. A. (2017). Reconciliation of pH_{25} and pH_{insitu} Acidification Rates of the Surface Oceans: A Simple Conversion Using Only *In Situ* Temperature. *Limnol. Oceanogr. Methods* 15 (3), 328–335. doi:10.1002/lom3.10170

Mekkes, L., Renema, W., Bednaršek, N., Alin, S. R., Feely, R. A., Huisman, J., et al. (2021). Pteropods Make Thinner Shells in the Upwelling Region of the California Current Ecosystem. *Sci. Rep.* 11 (1), 1731. doi:10.1038/s41598-021-81131-9

Millero, F. J. (2010). Carbonate Constants for Estuarine Waters. *Mar. Freshw. Res.* 61, 139–142. doi:10.1071/mf09254

Millero, F. J., Feistel, R., Wright, D. G., and McDougall, T. J. (2008). The Composition of Standard Seawater and the Definition of the Reference-Composition Salinity Scale. *Deep Sea Res. Oceanographic Res. Pap.* 55 (1), 50–72. doi:10.1016/j.dsr.2007.10.001

Moya, A., Howes, E. L., Lacoue-Labarthe, T., Forêt, S., Hanna, B., Medina, M., et al. (2016). Near-future pH Conditions Severely Impact Calcification, Metabolism and the Nervous System in the pteropod Heliconoides Inflatus. *Glob. Change Biol.* 22 (12), 3888–3900. doi:10.1111/gcb.13350

Mucci, A. (1983). The Solubility of Calcite and Aragonite in Seawater at Various Salinities, Temperatures, and One Atmosphere Total Pressure. *Am. J. Sci.* 283, 780–799. doi:10.2475/ajs.283.7.780

Orr, J. C., Fabry, V. J., Aumont, O., Bopp, L., Doney, S. C., Feely, R. A., et al. (2005). Anthropogenic Ocean Acidification over the Twenty-First Century and its Impact on Calcifying Organisms. *Nature* 437 (7059), 681–686. doi:10.1038/nature04095

Peck, V. L., Tarling, G. A., Manno, C., Harper, E. M., and Tynan, E. (2016). Outer Organic Layer and Internal Repair Mechanism Protects Pteropod Limacina Helicina from Ocean Acidification. *Deep Sea Res. Part Topical Stud. Oceanography* 127, 41–52. doi:10.1016/j.dsr2.2015.12.005

Pierrot, D., Lewis, E., and Wallace, D. W. R. (2006). "MS Excel Program Developed for CO_2 System Calculations," in *Carbon Dioxide Information Analysis Center* (Oak Ridge, Tennessee: Oak Ridge National Laboratory, U.S. Department of Energy, ORNL/CDIAC-105a).

Santos, I. R., Chen, X., Lecher, A. L., Sawyer, A. H., Moosdorf, N., Rodellas, V., et al. (2021). Submarine Groundwater Discharge Impacts on Coastal Nutrient Biogeochemistry. *Nat. Rev. Earth Environ.* 2, 307–323. doi:10.1038/s43017-021-00152-0

Shih, T.-T., Chang, J.-C., Hsu, M.-Y., and Shen, S.-M. (1991). The marine Terraces and Coral Reef Dating in Liu-Chiu Yu, Taiwan (In Chinses). *Geographical Res.* 17, 85–97.

Shirayama, Y., and Thornton, H. (2005). Effect of Increased Atmospheric CO_2 on Shallow Water marine Benthos. *J. Geophys. Res.* 110 (C9). doi:10.1029/2004JC002618

Talmage, S. C., and Gobler, C. J. (2010). Effects of Past, Present, and Future Ocean Carbon Dioxide Concentrations on the Growth and Survival of Larval Shellfish. *Proc. Natl. Acad. Sci.* 107 (40), 17246–17251. doi:10.1073/pnas.0913804107

Taniguchi, M., Dulai, H., Burnett, K. M., Santos, I. R., Sugimoto, R., Stieglitz, T., et al. (2019). Submarine Groundwater Discharge: Updates on its Measurement Techniques, Geophysical Drivers, Magnitudes, and Effects. *Front. Environ. Sci.* 7 (141). doi:10.3389/fenvs.2019.00141

Van de Waal, D. B., John, U., Ziveri, P., Reichart, G.-J., Hoins, M., Sluijs, A., et al. (2013). Ocean Acidification Reduces Growth and Calcification in a Marine Dinoflagellate. *PLoS One* 8 (6), e65987. doi:10.1371/journal.pone.0065987

Wang, G., Jing, W., Wang, S., Xu, Y., Wang, Z., Zhang, Z., et al. (2014). Coastal Acidification Induced by Tidal-Driven Submarine Groundwater Discharge in a Coastal Coral Reef System. *Environ. Sci. Technol.* 48 (22), 13069–13075. doi:10.1021/es5026867

Wang, S.-L., Chen, C.-T. A., Huang, T.-H., Tseng, H.-C., Lui, H.-K., Peng, T.-R., et al. (2018). Submarine Groundwater Discharge Helps Making Nearshore Waters Heterotrophic. *Sci. Rep.* 8 (1), 11650. doi:10.1038/s41598-018-30056-x

Weiss, R. F. (1981). Determinations of Carbon Dioxide and Methane by Dual Catalyst Flame Ionization Chromatography and Nitrous Oxide by Electron Capture Chromatography. *J. Chromatogr. Sci.* 19, 611–616. doi:10.1093/chromsci/19.12.611

Zhai, W. d., Zhao, H. d., Su, J. l., Liu, P. f., Li, Y. w., and Zheng, N. (2019). Emergence of Summertime Hypoxia and Concurrent Carbonate Mineral Suppression in the Central Bohai Sea, China. *J. Geophys. Res. Biogeosci.* 124 (9), 2768–2785. doi:10.1029/2019jg005120

Zhai, W. (2018). Exploring Seasonal Acidification in the Yellow Sea. *Sci. China Earth Sci.* 61 (6), 647–658. doi:10.1007/s11430-017-9151-4

Conflict of Interest: The authors declare that the research was conducted in the absence of any commercial or financial relationships that could be construed as a potential conflict of interest.